PHYSICAL REVIEW D **92,** 013005 (2015)

Radiative neutrino masses in the singlet-doublet fermion dark matter model with scalar singlets

Diego Restrepo,[*] Andrés Rivera,[†] Marta Sánchez-Peláez,[‡] and Oscar Zapata[§]

Instituto de Física, Universidad de Antioquia, Calle 70 No. 52-21, Apartado Aéreo 1226, Medellín, Colombia

Walter Tangarife[‖]

Department of Particle Physics, School of Physics and Astronomy, Tel Aviv University, Tel Aviv 69978, Israel

(Received 7 May 2015; published 9 July 2015)

When the singlet-doublet fermion dark matter model is extended with additional Z_2-odd real singlet scalars, neutrino masses and mixings can be generated at the one-loop level. In this work, we discuss the salient features arising from the combination of the two resulting simplified dark matter models. When the lightest Z_2-odd particle is a scalar singlet, $\mathrm{Br}(\mu \to e\gamma)$ could be measurable provided that the singlet-doublet fermion mixing is small enough. In this scenario, the new decay channels of vector-like fermions into scalars can also generate interesting leptonic plus missing transverse energy signals at the LHC. On the other hand, in the case of doublet-like fermion dark matter, scalar coannihilations lead to an increase in the relic density which allows one to lower the bound of doublet-like fermion dark matter.

DOI: 10.1103/PhysRevD.92.013005 PACS numbers: 14.60.Pq, 95.35.+d

I. INTRODUCTION

In view of the lack of signals of new physics in strong production at the LHC, there is a growing interest in simplified models where the production of new particles is only through electroweak processes, with lesser constraints from LHC limits. In particular, there are simple standard model (SM) extensions with dark matter (DM) candidates, such as the singlet scalar dark matter (SSDM) model [1–3], or the singlet-doublet fermion dark matter (SDFDM) model [4–9]. In this kind of models, the prospects for signals at the LHC are in general limited because of the softness of final SM particles coming from the small charged to neutral mass gaps of the new particles, which is usually required to obtain the proper relic density. In this sense, the addition of new particles, motivated for example by neutrino physics, could open new detection possibilities, either through new decay channels or additional mixings which increase the mass gaps.

Along these lines, scotogenic models [10]–which feature neutrino masses suppressed by the same mechanism that stabilizes dark matter—have been thoroughly studied with specific predictions in almost all of the current terrestrial and satellite detector experiments (for a review see, for example, Ref. [11]). The simplest models correspond to extensions of the inert doublet model [12,13] with extra singlet or triplet fermions. Recently, the full list of 35 scotogenic models with neutrino masses at one loop [14,15][1] and at most triplet representations of $\mathrm{SU}(2)_L$ was presented in Ref. [17] (and partially in Ref. [18]). The next to simplest scotogenic model is possibly the one where the role of the singlet fermions is played by singlet scalars, and the role of the scalar inert doublet is played by a vector-like doublet fermion. One additional singlet fermion is required to generate neutrino masses at the one-loop level. This kind of extension of the singlet dark matter model is labeled as the model T13A with $\alpha = 0$ in Ref. [17]. The extra fermion, which is required in order to have radiative neutrino masses, can be the singlet in the SDFDM model.

In the simplest scotogenic model [10], singlet fermion dark matter is possible but quite restricted by lepton flavor violation (LFV) [19,20]. In contrast, we will show that in the present model the region of the parameter space corresponding to fermion dark matter is well below the present and near-future constraints on $\mathrm{Br}(\mu \to e\gamma)$.

On the other hand, when the lightest Z_2-odd particle (LOP) is one of the scalar singlets, in the regions of the parameter space compatible with constraints from LFV we could have promising signals at colliders, thanks to the electroweak production of fermion doublets and possible large branchings into charged leptons.

The dark matter phenomenology of both the SSDM and SDFDM models has been extensively studied in the literature and recently revisited in Ref. [21]. Here, we consider the possible effect of coannihilations with the scalar singlets for fermion dark matter. We will see that these coannihilations tend to increase the relic density of

[*]restrepo@udea.edu.co
[†]afelipe.rivera@udea.edu.co
[‡]martal.sanchez@udea.edu.co
[§]oalberto.zapata@udea.edu.co
[‖]waltert@post.tau.ac.il

[1]The general realization of the Weinberg operator at two loops has been undertaken in Ref. [16].

dark matter and may modify the viable parameter space of the model. Specifically, they allow one to reduce the lower bound on the mass of the doublet-like dark matter particle from around 1100 GeV down to about 900 GeV.

The rest of the paper is organized as follows. In the next section, we present the model. Our main results are presented in Secs. III–VI, where we describe the correlation between the generation of neutrino masses and lepton flavor violation, new signals at colliders in the case of scalar dark matter, and new coannihilation possibilities in the case of singlet-doublet fermion dark matter. Finally, in Sec. VII we present our conclusions. In the Appendix, we present the analytic diagonalization formulas for the mass matrix of neutral fermions.

II. THE MODEL

The particle content of the model consists of two $\mathrm{SU}(2)_L$ doublets of Weyl fermions $\tilde{R}_u$, R_d with opposite hypercharges, one singlet Weyl fermion N of zero hypercharge, and a set of real scalar singlets S_α also of zero hypercharge. All of them are odd under one imposed Z_2 symmetry, under which the SM particles are even. The new particle content is summarized in Table I. The most general Z_2-invariant Lagrangian is given by

$$\begin{aligned}\mathcal{L} = \mathcal{L}_{\mathrm{SM}} &+ M_D \epsilon_{ab} R_d^a \tilde{R}_u^b - \frac{1}{2} M_N N N - h_{i\alpha} \epsilon_{ab} \tilde{R}_u^a L_i^b S_\alpha \\ &- \lambda_d \epsilon_{ab} H^a R_d^b N - \lambda_u \epsilon_{ab} \tilde{H}^a \tilde{R}_u^b N + \mathrm{H.c} \\ &- \left[\frac{1}{2}(M_S^2)_{\alpha\beta} S_\alpha S_\beta + \lambda_{\alpha\beta}^{\mathrm{SH}} \epsilon_{ab} \tilde{H}^a H^b S_\alpha S_\beta + \lambda_{\alpha\beta\gamma\delta}^{S} S_\alpha S_\beta S_\gamma S_\delta\right],\end{aligned} \tag{1}$$

where L_i are the lepton doublets, and we have defined the new $\mathrm{SU}(2)_L$ doublets in terms of left-handed Weyl fermions as

$$R_d = \begin{pmatrix} \psi_L^0 \\ \psi_L^- \end{pmatrix}, \qquad \tilde{R}_u = \begin{pmatrix} -(\psi_R^-)^\dagger \\ (\psi_R^0)^\dagger \end{pmatrix}$$

and $H = \begin{pmatrix} 0 & (h+v)/\sqrt{2} \end{pmatrix}^{\mathrm{T}}$ as the SM Higgs doublet with $\tilde{H} = i\sigma_2 H^*$ and $v = 246$ GeV. In the scalar potential, we assume that the $\mathbf{M}_S^2$ matrix has only positive entries and $(M_S^2)_{\alpha\beta} + \lambda_{\alpha\beta}^{\mathrm{SH}} v^2 = 0$ for $\alpha \neq \beta$, which means S_α are mass eigenstates with masses $m_{S_\alpha}^2 = (M_S^2)_{\alpha\alpha} + \lambda_{\alpha\alpha}^{\mathrm{SH}} v^2$ and $m_{S_\alpha} < m_{S_{\alpha+1}}$. On the other hand, the Z_2-odd fermion spectrum is composed of a charged Dirac fermion $\chi^- = (\psi_L^-, \psi_R^-)^T$ with a tree-level mass $m_{\chi^\pm} = M_D$, and three Majorana fermions arising from the mixture between the neutral parts of the $\mathrm{SU}(2)_L$ doublets and the singlet fermion. By defining the fermion basis through the vector $\Xi = (N, \psi_L^0, (\psi_R^0)^\dagger)^T$, the neutral fermion mass matrix reads

$$\mathbf{M}^\chi = \begin{pmatrix} M_N & -m_\lambda \cos\beta & m_\lambda \sin\beta \\ -m_\lambda \cos\beta & 0 & -M_D \\ m_\lambda \sin\beta & -M_D & 0 \end{pmatrix}, \tag{2}$$

where

$$m_\lambda = \frac{\lambda v}{\sqrt{2}}, \qquad \lambda = \sqrt{\lambda_u^2 + \lambda_d^2}, \qquad \tan\beta = \frac{\lambda_u}{\lambda_d}. \tag{3}$$

The specific signs on the right-hand side of Eq. (1) were chosen such that the terms in the mass matrix $\mathbf{M}^\chi$ follow the same convention of the bino-Higgsino sector in the neutralino mass matrix of the minimal supersymmetric standard model (MSSM) [22]. This convention facilitates the comparison between the present study and previous analyses regarding the bino-Higgsino DM limit of the MSSM. Such a limiting scenario occurs in the MSSM when the winos are decoupled from the spectrum and is accommodated within the SDFDM model when $m_\lambda = m_Z \sin\theta_W (\lambda = g'/\sqrt{2})$. The Majorana fermion mass eigenstates $\mathbf{X} = (\chi_1, \chi_2, \chi_3)^T$ are obtained through the rotation matrix $\mathbf{N}$ as $\Xi = \mathbf{N}\mathbf{X}$ such that

$$\mathbf{N}^{\mathrm{T}} \mathbf{M}^\chi \mathbf{N} = \mathbf{M}_{\mathrm{diag}}^\chi, \tag{4}$$

with $\mathbf{M}_{\mathrm{diag}}^\chi = \mathrm{Diag}(m_1^\chi, m_2^\chi, m_3^\chi)$ and m_n^χ being the corresponding masses (no mass ordering is implied). In what follows we assume CP invariance and therefore $\mathbf{N}$ can be chosen real. The analytical diagonalization of the neutral fermion mass matrix is carried out in the Appendix. For the subsequent analysis, it will be convenient to have some approximate expressions in the limit of small doublet-fermion mixing ($m_\lambda \ll M_D, M_N$). Expanding the analytical expressions for the eigensystem of Eq. (4) given in the Appendix, up to order m_λ^2, the fermion masses are

$$\begin{aligned} m_1^\chi &= M_N + \frac{M_D \sin(2\beta) + M_N}{M_N^2 - M_D^2} m_\lambda^2 + \mathcal{O}(m_\lambda^4), \\ m_2^\chi &= M_D + \frac{\sin(2\beta) + 1}{2(M_D - M_N)} m_\lambda^2 + \mathcal{O}(m_\lambda^4), \\ m_3^\chi &= -M_D + \frac{\sin(2\beta) - 1}{2(M_D + M_N)} m_\lambda^2 + \mathcal{O}(m_\lambda^4). \end{aligned} \tag{5}$$

TABLE I. α set of scalars and Weyl fermions of the model.

Symbol	$(\mathrm{SU}(2)_L, \mathrm{U}(1)_Y)$	Z_2	Spin
S_α	(1,0)	−	0
N	(1,0)	−	1/2
$\tilde{R}_u$,	$(2,+1/2)$	−	1/2
R_d	$(2,-1/2)$	−	1/2

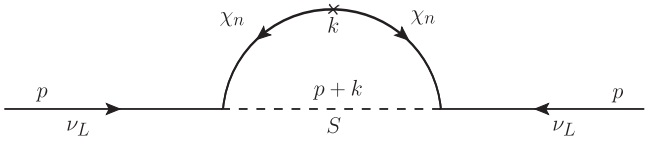

FIG. 1. One-loop Weyl-spinor Feynman rules [29] for the contributions to the neutrino mass, with three Majorana fermions ($n = 1, 2, 3$) and a singlet scalar S.

Approximate expressions for the mixing matrix are also given in the Appendix.

III. ONE-LOOP NEUTRINO MASSES

By assigning a null lepton number to the new fields in the model[2], the only lepton-number-violating term in the Lagrangian (1) is the one with the coupling $h_{i\alpha}$. Hence, the introduction of real singlet scalars allows one to generate nonzero neutrino masses at the one-loop level through the diagram shown in Fig. 1. The resulting one-loop neutrino mass matrix was presented in the interaction basis in Refs. [15] and [23], and more recently in the limit $\lambda_d = 0$ and $M_N \to 0$ in Ref. [24]. Instead, we work out the calculations in the more convenient mass eigenstate basis, in which the neutrino mass matrix takes the form

$$M^{\nu}_{ij} = -\sum_{\alpha} \frac{h_{i\alpha} h_{j\alpha}}{16\pi^2} \sum_{n=1}^{3} (N_{3n})^2 m_{\chi_n} B_0(0; m^2_{\chi_n}, m^2_{S_\alpha}), \quad (6)$$

where $B_0(0; m^2_{\chi_n}, m^2_{S_\alpha})$ is the B_0 Passarino-Veltman function [25] and (N_{mn}) are matrix elements of the rotation matrix $\mathbf{N}$. By using the identity

$$\sum_{n=1}^{3} (N_{3n})^2 m^{\chi}_n = (\mathbf{M}^{\chi})_{33} = 0, \quad (7)$$

we obtain the expected cancellation of divergent terms coming from the mass-independent term in B_0, leading to the finite neutrino mass matrix

$$M^{\nu}_{ij} = \sum_{\alpha} \frac{h_{i\alpha} h_{j\alpha}}{16\pi^2} \sum_{n=1}^{3} (N_{3n})^2 m_{\chi_n} f(m_{S_\alpha}, m_{\chi_n}) \quad (8)$$

$$= \sum_{\alpha} h_{i\alpha} \Lambda_{\alpha} h_{j\alpha} \quad (9)$$

$$= (\mathbf{h} \Lambda \mathbf{h}^{\mathrm{T}})_{ij}, \quad (10)$$

with $f(m_1, m_2) = (m_1^2 \ln m_1^2 - m_2^2 \ln m_2^2)/(m_1^2 - m_2^2)$, $\Lambda = \mathrm{Diag}(\Lambda_1, \Lambda_2, \Lambda_3)$, and

$$\Lambda_{\alpha} = \frac{1}{16\pi^2} \sum_{n=1}^{3} (N_{3n})^2 m_{\chi_n} f(m_{S_\alpha}, m_{\chi_n}). \quad (11)$$

The flavor structure of the neutrino mass matrix M^{ν}_{ij}, given by Eq. (9), allows us to express the Yukawa couplings in terms of the neutrino oscillation observables (ensuring the proper compatibility with them) through the Casas-Ibarra parametrization introduced in Refs. [26,27]. Thus, by using an arbitrary complex orthogonal rotation matrix $\mathcal{R}$, the Yukawa couplings $h_{i\alpha}$ are given by

$$\mathbf{h}^T = \mathbf{D}_{\sqrt{\Lambda^{-1}}} \mathcal{R} \mathbf{D}_{\sqrt{m_\nu}} \mathbf{U}^{\dagger}, \quad (12)$$

where $\mathbf{D}_{\sqrt{m_\nu}} = \mathrm{Diag}(\sqrt{m_{\nu 1}}, \sqrt{m_{\nu 2}}, \sqrt{m_{\nu 3}})$, $\mathbf{D}_{\sqrt{\Lambda^{-1}}} = \mathrm{Diag}(\sqrt{\Lambda_1^{-1}}, \sqrt{\Lambda_2^{-1}}, \ldots)$ and $\mathbf{U}$ is the Pontecorvo-Maki-Nakagawa-Sakata [28] neutrino mixing matrix. Henceforth we will consider the case of three scalar singlets, $\alpha = 1, 2, 3$, where the Yukawa couplings take the form

$$h_{i\alpha} = \frac{\sqrt{m_{\nu 1}} \mathcal{R}_{\alpha 1} U^*_{i1} + \sqrt{m_{\nu 2}} \mathcal{R}_{\alpha 2} U^*_{i2} + \sqrt{m_{\nu 3}} \mathcal{R}_{\alpha 3} U^*_{i3}}{\sqrt{\Lambda_\alpha}}. \quad (13)$$

In the above equation, the 3×3 matrix $\boldsymbol{\mathcal{R}}$ can be cast in terms of three rotation angles $\theta_{23}, \theta_{13}, \theta_{12}$, which are assumed to be real. It is worth mentioning that for the case with two scalar singlets $\alpha = 1, 2$ a viable scenario is also possible with the remark that one massless neutrino is obtained. To fully exploit the generality of the $h_{i\alpha}$ couplings obtained from Eq. (13), we stick to the case with three scalar singlets.

In summary, the set of input parameters of the model are the scalar masses m_{S_α}, M_N, M_D, λ, $\tan\beta$, the lightest neutrino mass $m_{\nu 1}$, and the three rotation angles present in $\boldsymbol{\mathcal{R}}$ and $\lambda^{\mathrm{SH}}_{\alpha\beta}$[3]. Without loss of generality we assume the latter are small, $\lambda^{\mathrm{SH}}_{\alpha\beta} \lesssim 0.01$, except for the case of scalar dark matter where $\lambda^{\mathrm{SH}}_{11}$ is set to give the proper relic density.

In order to have an approximate expression for Λ_α in terms of this set of input parameters, we can use the identity (7) to obtain

$$\Lambda_{\alpha} = \frac{1}{16\pi^2} \{ N^2_{31} m^{\chi}_1 [f(m_{S_\alpha}, m^{\chi}_1) - f(m_{S_\alpha}, m^{\chi}_3)] + N^2_{32} m^{\chi}_2 [f(m_{S_\alpha}, m^{\chi}_2) - f(m_{S_\alpha}, m^{\chi}_3)] \}.$$

The expression for the matrix elements N^2_{31} at $\mathcal{O}(m^2_\lambda)$ are given in the Appendix. Since N^2_{31} and $f(m_{S_\alpha}, m^{\chi}_2) - f(m_{S_\alpha}, m^{\chi}_3)$ are already $\mathcal{O}(m^2_\lambda)$, we can use the leading-order values for the other masses and mixing parameters to obtain

[2] If (instead of real singlets) complex singlets were considered, a conserved lepton number would have been obtained in the Lagrangian, and in such a case vanishing neutrino masses are obtained.

[3] The couplings $\lambda^{S}_{\alpha\beta\gamma\delta}$ are irrelevant for phenomenological purposes.

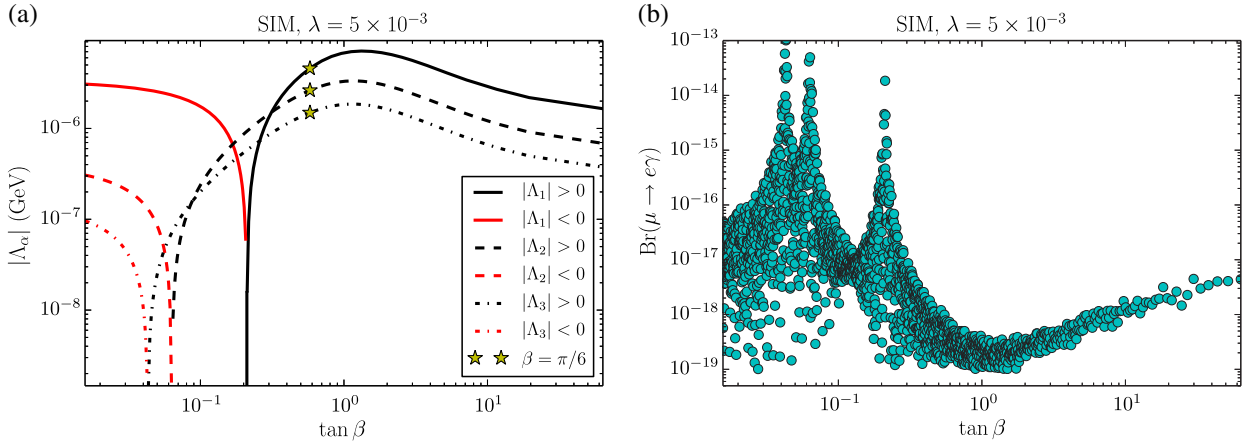

FIG. 2 (color online). $\tan\beta$ dependence of (a) Λ_a and (b) $\mathrm{Br}(\mu \to e\gamma)$, for the set of input masses in Eq. (15) with $\lambda = 5 \times 10^{-3}$.

$$\Lambda_\alpha \approx \frac{1}{16\pi^2}\left\{N_{31}^2 M_N[f(m_{S_\alpha}, M_N) - f(m_{S_\alpha}, M_D)] + \frac{1}{2}M_D[f(m_{S_\alpha}, m_2^\chi) - f(m_{S_\alpha}, m_3^\chi)]\right\} + \mathcal{O}(m_\lambda^4).$$

With the last two approximate formulas for masses in Eq. (5), and the N_{31}^2 mixing in Eq. (A7), we have

$$16\pi^2 \frac{\Lambda_\alpha}{m_\lambda^2} \approx \left(\frac{M_D \cos\beta + M_N \sin\beta}{M_D^2 - M_N^2}\right)^2 M_N[f(m_{S_\alpha}, M_N) - f(m_{S_\alpha}, M_D)] + \frac{M_D^2[M_D \sin(2\beta) + M_N]}{(M_D^2 - M_N^2)(M_D^2 - m_{S_\alpha}^2)^2}\left\{M_D^2 - m_{S_\alpha}^2\left[\log\left(\frac{M_D^2}{m_{S_\alpha}^2}\right) + 1\right]\right\} + \mathcal{O}(m_\lambda^2). \quad (14)$$

To illustrate the dependence on $\tan\beta$ of Λ_α, we consider the following set of input masses (SIM) compatible with singlet scalar dark matter:

$$m_{S_1} = 60\ \text{GeV}, \qquad m_{S_2} = 800\ \text{GeV}, \qquad m_{S_3} = 1500\ \text{GeV}, \qquad m_N = 100\ \text{GeV}, \qquad m_D = 550\ \text{GeV}. \quad (15)$$

The results for $\lambda = 5 \times 10^{-3}$ are shown in Fig. 2(a). For large values of $\tan\beta$, the Λ_α are positive. However, there are specific values of $\tan\beta$ for which each Λ_α goes to zero and turns to negative values, as illustrated by the red lines in the plot. The specific point with $\beta = \pi/6$ is depicted by the yellow stars in the figure.

IV. LEPTON FLAVOR VIOLATION

The size of the LFV is controlled by the lepton-number-violating couplings $h_{i\alpha}$. From the approximate expression for Λ_α in Eq. (14) and the analysis of the previous section, we will show that these couplings are inversely related to the Yukawa coupling strength λ. Since in SDFDM the observed dark matter abundance is typically obtained for $\lambda \gtrsim 0.1$ [9], the lepton flavor observables are not expected to give better constraints than the ones obtained from direct-detection experiments. Therefore, we will focus our discussion of LFV in regions of the parameter space where S_1 is the dark matter candidate.

It is well known that LFV processes put severe constraints on the LFV couplings and, in general, on the model's parameter space. One of the most restrictive LFV processes is the radiative muon decay $\mu \to e\gamma$, which in the present model is mediated by the same particles that are present in the internal lines of the one-loop neutrino mass diagram. The corresponding expression for the branching ratio reads

$$\mathrm{Br}(\mu \to e\gamma) = \frac{3}{4}\frac{\alpha_{\mathrm{em}}}{16\pi G_F^2}\left|\sum_\alpha h_{1\alpha}\frac{F(M_D^2/m_{S_\alpha}^2)}{m_{S_\alpha}^2}h_{2\alpha}^*\right|^2, \quad (16)$$

where

$$F(x) = \frac{x^3 - 6x^2 + 3x + 2 + 6x\ln x}{6(x-1)^4}. \quad (17)$$

With the implementation of the model in the BSM-TOOLBOX [30] of SARAH [31,32], we have cross-checked the one-loop results for both neutrino masses and $\mathrm{Br}(\mu \to e\gamma)$. Moreover, with the SARAH FLAVORKIT [33], we have also checked that the most restrictive lepton-flavor-violating process in the scan, to be described below, is just $\mathrm{Br}(\mu \to e\gamma)$. From Eqs. (9) and (12), we obtain

$$M^{\nu}_{12} = \sum_{\alpha} h_{1\alpha}\Lambda_{\alpha}h_{2\alpha} = [\mathbf{U}^{*}\mathbf{M}^{\nu}_{\rm diag}\mathbf{U}^{\dagger}]_{12}. \qquad (18)$$

Comparing this result with the corresponding combination of couplings in the expression for $\mathrm{Br}(\mu \to e\gamma)$ in Eq. (16), we expect that for a set of fixed input masses $\mathrm{Br}(\mu \to e\gamma)$ turns out to be inversely proportional to Λ_{α}^2. This is illustrated in Fig. 2(b) for $\lambda = 5 \times 10^{-3}$, where the scatter plot of $\mathrm{Br}(\mu \to e\gamma)$ is shown for the same range of $\tan\beta$ values as the one in Fig. 2(a). In such a case, once $h_{i\alpha}$ are obtained from the Casas-Ibarra parametrization, the specific hierarchy of Λ_{α} fixes the several contributions to $\mathrm{Br}(\mu \to e\gamma)$. The dispersion of the points is due to the 3σ variation of neutrino oscillation data [34] used in the numerical implementation of the Casas-Ibarra parametrization, along with the random variation of the parameters of $\mathcal{R}$. The minimum value of $\mathrm{Br}(\mu \to e\gamma)$ around $\tan\beta = 1$ corresponds to the maximum value of Λ_{α}, while the maximum values happen at the cancellation points of each Λ_{α}. In the subsequent analysis, and for a fixed SIM and λ, we allow for cancellations only by 2 orders of magnitude from the maximum value of each Λ_{α}.

The full scan of the input masses up to 2 TeV, with $m_{S_1} > 53$ GeV [21] as the dark matter candidate, $M_D > 100$ GeV to satisfy LEP constraints, and $10^{-2} \leq \tan\beta \leq 10^{2}$, gives rise to the dark gray plus light gray regions in Fig. 3. In particular, the λ variation for the SIM with $\beta = \pi/6$, denoted by yellow stars in Fig. 2(a), is illustrated with the white dots in Fig. 3. The corresponding dashed line is obtained for the best-fit values of the neutrino oscillation data and with $\mathcal{R}$ fixed to the identity. The horizontal dotted line in the plot corresponds to the current experimental bound for $\mathrm{Br}(\mu \to e\gamma) < 5.7 \times 10^{-13}$ at 90% C.L. [35]. The upper part of the light gray region is restricted by our imposition to avoid too strong a cancellation in Λ_{α}. For all of the sets of input masses in the random scan, we check that this cancellation region always happens when $\tan\beta < 1$. In this way, points with $\tan\beta > 1$ are absent from the light gray region, as labeled in Fig. 3. For the same reason, in the dark gray region there are no points with $\Lambda_{\alpha} \ll \Lambda_{\beta} \sim \Lambda_{\gamma} (\alpha \neq \beta \neq \gamma)$. We can check, for example, that points with $\Lambda_1 \ll \Lambda_2 < \Lambda_3$ are absent inside the dark gray region of Fig. 3.

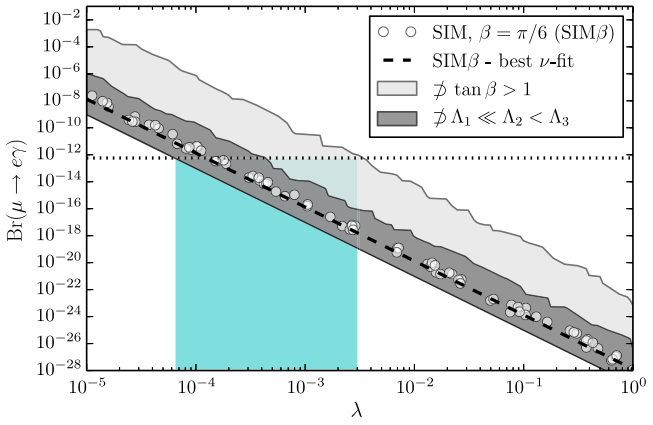

FIG. 3 (color online). $\mathrm{Br}(\mu \to e\gamma)$ in terms of the Yukawa coupling strength λ for the SIM in Eq. (15) with $\beta = \pi/6$, and the general scan described in the text.

The lower part of the dark gray region is saturated by the values of $M_D = 2$ TeV, and gives rise to the lower bound $\lambda \gtrsim 6 \times 10^{-5}$. With our restriction on the cancellation of Λ_{α}, points in the scan with $\lambda \lesssim 3 \times 10^{-3}$ can be excluded from the $\mathrm{Br}(\mu \to e\gamma)$ limit.

V. COLLIDER PHENOMENOLOGY

The LHC phenomenology in the case of the singlet-doublet fermion dark matter was already analyzed in Ref. [21]. They concluded that the recast of the current LHC data is easier to evade, but the long-run prospects are promising, since the region $M_N, m_{\lambda} \ll M_D$ could be probed up to $M_D \lesssim 600$–700 GeV for the 14 TeV run of the LHC with 3000 fb^{-1}.

On the other hand, in the case of the singlet scalar dark matter, the main production processes associated with the new fermions remain the same, but there are new signals from the mediation (or the presence in the final decay chains) of the new scalars. The most promising possibility is the dilepton plus missing transverse energy signal coming from the production of charged fermions decaying into leptons and the lightest scalar. This signal can be important when λ is not too large, $\lambda \lesssim 0.1$, and $M_N \gtrsim M_D$. For a fixed set of input parameters, the random phases in the Casas-Ibarra parametrization can be chosen to have all the possibilities in the lepton flavor space associated with the coupling h_{i1}, with $i = e, \mu, \tau$. In view of that, we will focus on the best scenario where $\mathrm{Br}(\chi^{\pm} \to l^{\pm}S_1) \approx 1$ ($l^{\pm} = e^{\pm}$ or $\mu^{\pm}$). The Feynman diagram for the processes is displayed in Fig. 4.

The mass of the charged Dirac fermion $\chi^{\pm}$ can be constrained from dilepton plus missing transverse energy searches at the LHC. In Ref. [36], this kind of signals was used by the ATLAS Collaboration to establish bounds on the slepton masses from the search for $pp \to \tilde{l}^{+}\tilde{l}^{-} \to l^{+}l^{-}\tilde{\chi}^{0}\tilde{\chi}^{0}$, where $\tilde{\chi}^{0}$ are the neutralinos, and the same

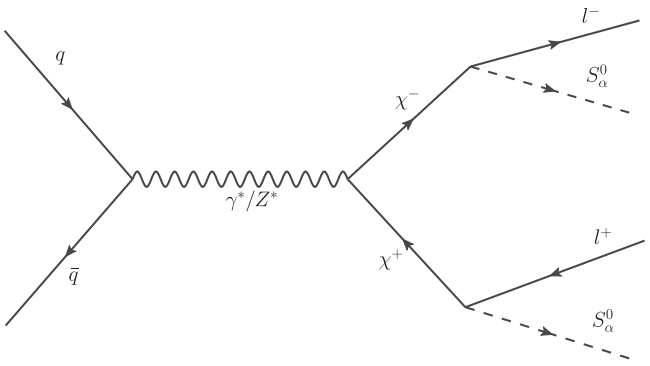

FIG. 4. Feynman diagram for $pp \to \chi^{+}\chi^{-} \to l^{+}l^{-}S_{\alpha}S_{\alpha}$.

exclusion is reported for $l = e$ or μ. Purely left-handed sleptons produced and decaying this way have been excluded up to masses of about 300 GeV at 95% C.L., from the data with an integrated luminosity of 20.3 fb^{-1} and a pp collision energy of 8 TeV. This corresponds to an excluded cross section of 1.4 fb at next-to-leading order (NLO) calculated with PROSPINO [37].

In the present model, the charged fermion field may decay in the mode $\chi^{\pm} \to e_i^{\pm} S_1$ which are proportional to the Yukawa couplings h_{i1}. Therefore, a similar final state as in the slepton pair production is obtained through the process $pp \to \chi^+\chi^- \to l^+l^- S_1 S_1$, as can be seen in Fig. 4.

In this case, the excluded cross section of this process can be estimated from

$$\sigma(pp \to l^+l^- S_1 S_1) = \sigma(pp \to \chi^+\chi^-) \times \mathrm{Br}(\chi^{\pm} \to l^{\pm} S_1)^2, \tag{19}$$

where $\sigma(pp \to \chi^+\chi^-)$ is the pair-production cross section of the charged Dirac fermion, and $\mathrm{Br}(\chi^{\pm} \to l^{\pm} S_1)$ is the branching fraction for the $\chi^{\pm} \to l^{\pm} S_1$ mode.

The pair production of charged Dirac fermions can be calculated in the pure-Higgsino limit of the minimal supersymmetric standard model. The NLO cross section calculated with PROSPINO is displayed in Fig. 5 as a function of the charged Dirac fermion.

For points in the parameter space where the Casas-Ibarra solution is chosen such that $\mathrm{Br}(\chi^{\pm} \to l^{\pm} S_1) \approx 1$, and assuming the same efficiency as for the dilepton plus missing transverse energy signal coming from left sleptons in Eq. (19), the charged Dirac fermions of the present model can be excluded up to 510 GeV, as illustrated in Fig. 5.

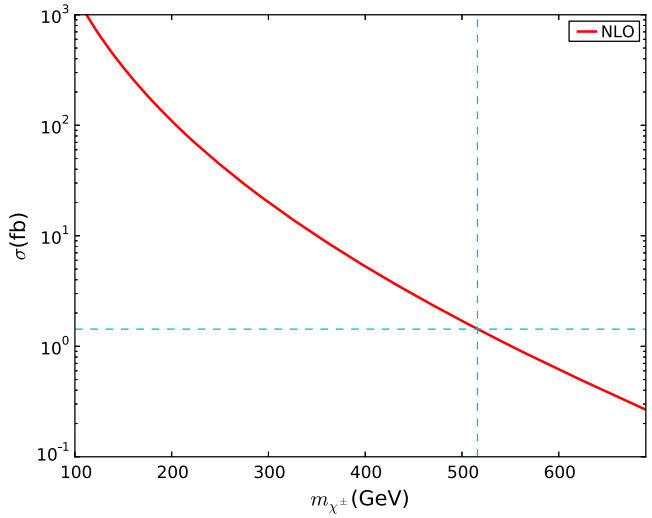

FIG. 5 (color online). NLO cross section for the charged Dirac fermion pair production at the LHC with pp collisions at $\sqrt{s} = 8$ TeV. The horizontal dashed line for the excluded cross section of 1.4 fb corresponds to a mass about of 510 GeV, which is illustrated by the vertical dashed line.

Note that many points in the scan of Fig. 3 with $\lambda \lesssim 0.1$ and featuring $m_{S_1} \ll M_D$ could be excluded by this LHC constraint. However, a detailed analysis of the restriction from Run I of the LHC, in the full parameter space of the model, is beyond the scope of this work.

VI. SINGLET-DOUBLET FERMION DARK MATTER

In this model, the role of the dark matter particle can be played by either the lightest of the fermions χ_{LOP} or the lightest of the scalars S_1. In the latter case, the present model resembles the singlet scalar DM model [1–3] as long as the other Z_2-odd particles do not contribute to the total annihilation cross section of S_1, namely through the addition of new (co)annihilation channels. Therefore, by choosing a nondegenerate mass spectrum and small Yukawa couplings (which is in agreement with neutrino masses) the effects of these particles on dark matter can be neglected. Hence, we expect the dark matter phenomenology to be similar to that of the SSDM [38].

On the other hand, regarding the case of fermion DM, the present model includes the singlet-doublet fermion DM model [4–9]. In such a scenario, when the dark matter candidate is mainly singlet (doublet), the relic density is in general rather large (small). In particular, a pure doublet has the proper relic density for $M_D \sim 1$ TeV [5,9,39] with decreasing values as M_D decreases. Nonetheless, in the present model we have the additional possibility of coannihilations between the Z_2-odd scalars and fermions. In this work, we explore to what extent coannihilation with scalars may allow one to recover pure-doublet DM regions with $M_D \lesssim 1$ TeV and $\lambda \lesssim 0.3$, while keeping the proper relic density. Hereafter, we focus on this specific region.

In the simple radiative seesaw model with inert doublet scalar dark matter, the coannihilations with singlet fermions can enhance (rather than reduce) the relic density, as shown in Ref. [40]. That work also presented a review of several models [41–45] where such an enhancement also occurs. In particular, supersymmetric models where the neutralino is Higgsino like were considered in Ref. [45] and it was shown that slepton coannihilations not only lead to an increase in the relic density, but also to an enhancement in the predicted indirect-detection signals. Below, we show that the singlet scalars can play the role of the sleptons in our generalization of the Higgsino-like dark matter with radiative neutrino masses.

The interactions of the scalars S_α are described by the $h_{i\alpha}$, $\lambda^{\mathrm{SH}}_{\alpha\beta}$ terms in Eq. (1). It turns out that Yukawa interactions are suppressed by neutrino masses ($h_{i\alpha} \lesssim 10^{-4}$) and the same occurs for the interaction with the Higgs boson if we impose $\lambda^{\mathrm{SH}}_{\alpha\beta} \lesssim 10^{-2}$. In this way, the coannihilating scalars S_α act as parasite degrees of freedom at freeze-out, leading to an increase of the singlet-doublet fermion relic density.

By following the discussion in Ref. [40], the maximum enhancement of the relic density is achieved when $\Delta_{S_\alpha} = (m_{S_\alpha} - m^{\chi}_{\rm LOP})/m^{\chi}_{\rm LOP}$ becomes negligible. Accordingly, one can write

$$\frac{\Omega^{S_\alpha}}{\Omega^0} \approx \left(\frac{g_0 + g_{S_\alpha}}{g_0}\right)^2, \tag{20}$$

where $\Omega^{S_\alpha}(\Omega^0)$ denotes the relic density with (without) S_α coannihilations, g_{S_α} represents the total number of internal degrees of freedom related to the scalars participating in the coannihilation process, and g_0 is the total number of internal degrees of freedom when $\Delta_{S_\alpha} \gg 1$. When the DM particle is pure doublet ($M_D \sim 1$ TeV and $M_N \gg M_D$), the fermion masses are $m^{\chi}_1 = M_N, m^{\chi}_{2,3} \approx m_{\chi^\pm} = M_D$, and therefore $g_0 = g_{\chi_2} + g_{\chi_3} + g_{\chi^\pm} = 8$. Since each real scalar has one degree of freedom, we have $g_{S_\alpha} = 1, 2, 3$ depending on the number of scalars coannihilating. Thus, it follows that the maximum enhancement is $\Omega^{S_\alpha}/\Omega^0 = 1.27, 1.56, 1.89$, respectively. This enhancement results in that—for the present model with doublet-like DM and $\lambda \lesssim 0.3$—the M_D required to explain the correct relic density lies in the range [0.9, 1.1] TeV, instead of taking a single value as in the SDFDM model. The values inside this range arise due to the lack of mass degeneracy between the fermions and scalars. In Fig. 6, we show the effect of coannihilations on the relic density[4] of $m^{\chi}_{\rm LOP}$ for a mass degeneracy of 0.1 to 10% between scalar singlets and the DM candidate and for $\lambda = 0.3$ and $\tan\beta = 2$. In particular, in the light gray region we plot the coannihilations with two scalars to facilitate the comparison with the results in Ref. [45] for Higgsino-like dark matter coannihilating with a right-handed stau ($g \approx 2$ in their plots). As expected, the upper limit in the LOP mass is about 20% smaller with respect to the case without coannihilation, and we could expect similar enhancements for indirect DM searches as in Ref. [45] for $g \approx 2$. Note that, when $M_D, M_N < 1$ TeV, the impact of the S_α coannihilation is reduced because, in such a case, the dark matter particle is a mixture of singlet and doublet (well-tempered DM [49]), and the non-negligible splitting among the fermion particles χ leads to a nonzero Boltzmann suppression. We have checked that the same results are obtained when $\lambda \lesssim 0.3$.

With regard to DM direct detection in the pure-doublet DM scenario discussed above, it is not restricted by the current LUX [50] bounds as long as $\tan\beta > 0$. This is due to the existence of zones—known as blind spots—where the spin-independent cross section vanishes identically, and they occur only for positive values of $\tan\beta$ [9].[5] As a consequence, the recovered pure-doublet DM regions are still viable in light of the present results of direct searches for dark matter.

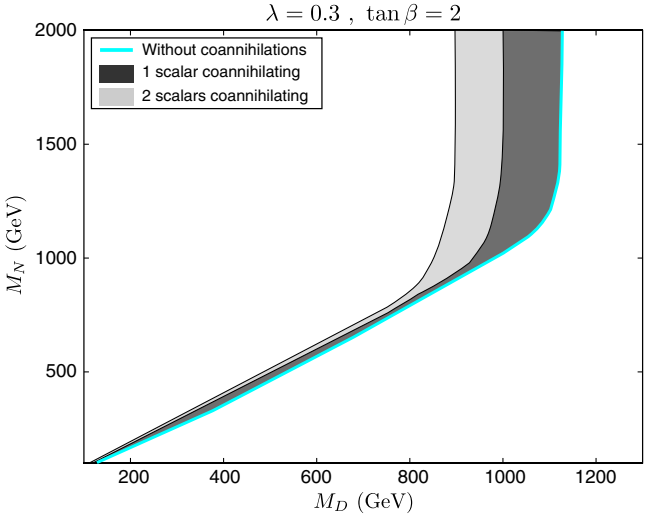

FIG. 6 (color online). Regions consistent with the observed relic density for $\lambda = 0.3$ and $\tan\beta = 2$. The solid cyan line corresponds to the observed relic density without coannihilations, which were shown to be compatible with the current direct-detection bounds from LUX [50] in Ref. [9]. The effect of the coannihilations with the new scalars is shown for a mass degeneracy of 0.1 to 10% between the scalars and the DM candidate. The dark gray region corresponds to coannihilations with one scalar singlet, while the dark plus light gray regions correspond to coannihilations with two scalar singlets.

VII. CONCLUSIONS

We have combined the SDFDM and SSDM models into a framework that generates radiative neutrino masses. The required lepton number violation only happens if the scalars are real. We have then explored the novel features of the final model in flavor physics, collider searches, and dark matter-related experiments. In the case of SSDM, for example, the singlet-doublet fermion mixing cannot be too small in order to be compatible with LFV observables like $\mathrm{Br}(\mu \to e\gamma)$, while in the case of fermion dark matter the LFV constraints are automatically satisfied. The presence of new decay channels for the next-to-lightest odd particle opens the possibility of new signals at the LHC. In particular, when the singlet scalar is the lightest odd particle and the singlet-like Majorana fermion is heavier than the charged Dirac fermion, the production of the latter yields dilepton plus missing transverse energy signals. For large enough $e^\pm$ or $\mu^\pm$ branchings, these signals could exclude charged Dirac fermion masses of order 500 GeV in Run I of the LHC. Finally, the effect of coannihilations with the scalar singlets was studied in the case of doublet-like fermion dark matter. In that case, it is possible to obtain the observed dark matter relic density with lower values of the LOP mass.

[4]The relic density is calculated with the BSM-TOOLBOX chain: SPHENO 3.3.6 [46]- MICROMEGAS 4.1.7 [47,48].

[5]Note that $\tan\beta > 0$ corresponds to $\tan\theta < 0$ in the notation of Ref. [9].

ACKNOWLEDGMENTS

We are very grateful to Camilo García Cely, Enrico Nardi, Federico von der Pahlen, and especially to Carlos Yaguna for their illuminating discussions. D. R. and O. Z. have been partially supported by UdeA through the grants Sostenibilidad-GFIF, CODI-2014-361 and CODI-IN650CE, and COLCIENCIAS through the Grants No. 111-556-934918 and 111-565-842691. W. T. has been supported by grants from ISF (1989/14), US-Israel BSF (2012383), and GIF (I-244-303.7-2013).

APPENDIX: ANALYTIC FORMULAS FOR MASSES AND MIXING MATRIX OF NEUTRAL FERMIONS

The characteristic equation of the mass matrix (2) is [9][6]

$$[(M^{\chi}_{\rm diag})^2_{ii} - M_D^2][M_N - (M^{\chi}_{\rm diag})_{ii}] + \frac{1}{2}m_\lambda^2[(M^{\chi}_{\rm diag})_{ii} + M_D \sin 2\beta] = 0.$$

The solutions to the cubic equation in $(M^{\chi}_{\rm diag})_{ii}$ are

$$m_1^{\chi} = z_2 + \frac{M_N}{3}, \qquad m_2^{\chi} = z_1 + \frac{M_N}{3}, \qquad m_3^{\chi} = z_3 + \frac{M_N}{3}, \tag{A1}$$

where

$$\begin{aligned}
z_1 &= \left(-\frac{q}{2} + \sqrt{\frac{q^2}{4} + \frac{p^3}{27}}\right)^{1/3} + \left(-\frac{q}{2} - \sqrt{\frac{q^2}{4} + \frac{p^3}{27}}\right)^{1/3},\\
z_2 &= -\frac{z_1}{2} + \sqrt{\frac{z_1^2}{4} + \frac{q}{z_1}},\\
z_3 &= -\frac{z_1}{2} - \sqrt{\frac{z_1^2}{4} + \frac{q}{z_1}},\\
p &= -\frac{1}{3}M_N^2 - (M_D^2 + m_\lambda^2),\\
q &= -\frac{2}{27}M_N^3 - \frac{1}{3}M_N(M_D^2 + m_\lambda^2) + [M_N M_D^2 - m_\lambda^2 \sin(2\beta) M_D].
\end{aligned} \tag{A2}$$

Notice that $q^2/4 + p^3/27 < 0$ and therefore we have three real masses m_i^{χ} $(i = 1, 2, 3)$.

Expanding the eigensystem in Eq. (4) by assuming that $N_{1i} \neq 0$, we have

$$\begin{aligned}
M_{21}^{\chi}\frac{N_{2i}}{N_{1i}} + M_{31}^{\chi}\frac{N_{3i}}{N_{1i}} &= -(M_{11}^{\chi} - m_i^{\chi}),\\
(M_{22}^{\chi} - m_i^{\chi})\frac{N_{2i}}{N_{1i}} + M_{32}^{\chi}\frac{N_{3i}}{N_{1i}} &= -M_{12}^{\chi},\\
M_{23}^{\chi}\frac{N_{2i}}{N_{1i}} + (M_{33}^{\chi} - m_i^{\chi})\frac{N_{3i}}{N_{1i}} &= -M_{13}^{\chi},
\end{aligned}$$

where

$$N_{1i} = \left[1 + \left(\frac{N_{2i}}{N_{1i}}\right)^2 + \left(\frac{N_{3i}}{N_{1i}}\right)^2\right]^{-1/2}. \tag{A3}$$

Using the matrix $\mathbf{M}^{\chi}$ given in Eq. (2), we get the ratios

$$\begin{aligned}
\frac{N_{2i}}{N_{1i}} &= -\frac{m_\lambda \cos\beta}{m_i^{\chi}} + \frac{M_D}{m_i^{\chi}}\frac{[m_i^{\chi}(M_N - m_i^{\chi}) + m_\lambda^2 \cos\beta^2]}{m_\lambda(m_i^{\chi}\sin\beta + M_D\cos\beta)},\\
\frac{N_{3i}}{N_{1i}} &= -\frac{[m_i^{\chi}(M_N - m_i^{\chi}) + m_\lambda^2\cos\beta^2]}{m_\lambda(m_i^{\chi}\sin\beta + M_D\cos\beta)}.
\end{aligned} \tag{A4}$$

1. Approximate mixing matrix

By using the analytical expressions for the mixing ratios of Eq. (A4) with the approximate eigenvalues (5) in Eq. (A3), we obtain

$$\begin{aligned}
N_{11}^2 &= 1 - \frac{[M_D^2 + M_N^2 + 2M_D M_N \sin(2\beta)]m_\lambda^2}{(M_D^2 - M_N^2)^2} + \mathcal{O}(m_\lambda^4),\\
N_{12}^2 &= \frac{[\sin(2\beta) + 1]m_\lambda^2}{2(M_N - M_D)^2} + \mathcal{O}(m_\lambda^4),\\
N_{13}^2 &= -\frac{[\sin(2\beta) - 1]m_\lambda^2}{2(M_D + M_N)^2} + \mathcal{O}(m_\lambda^4),
\end{aligned} \tag{A5}$$

[6]The analytic formulas for the neutralino masses and the neutralino mixing matrix were analyzed in Ref. [51].

$$
\begin{aligned}
N_{21}^2 &= \frac{m_\lambda^2(\sin\beta M_D + \cos\beta M_N)^2}{(M_N^2 - M_D^2)^2} + \mathcal{O}(m_\lambda^4),\\
N_{22}^2 &= \frac{1}{2} - \frac{m_\lambda^2(\sin\beta + \cos\beta)[\cos\beta M_N - \sin\beta(M_N - 2M_D)]}{4M_D(M_N - M_D)^2} + \mathcal{O}(m_\lambda^4),\\
N_{23}^2 &= \frac{1}{2} + \frac{m_\lambda^2(\cos\beta - \sin\beta)[\sin\beta(2M_D + M_N) + \cos\beta M_N]}{4M_D(M_D + M_N)^2} + \mathcal{O}(m_\lambda^4),
\end{aligned}
\tag{A6}
$$

$$
\begin{aligned}
N_{31}^2 &= \left(\frac{M_D\cos\beta + M_N\sin\beta}{M_N^2 - M_D^2}\right)^2 m_\lambda^2 + \mathcal{O}(m_\lambda^4),\\
N_{32}^2 &= \frac{1}{2} - \frac{[M_N\sin\beta - (M_N - 2M_D)\cos\beta](\cos\beta + \sin\beta)}{4M_D(M_N - M_D)^2} m_\lambda^2 + \mathcal{O}(m_\lambda^4),\\
N_{33}^2 &= \frac{1}{2} - \frac{[M_N\sin\beta + (M_N + 2M_D)\cos\beta](\cos\beta - \sin\beta)}{4M_D(M_N + M_D)^2} m_\lambda^2 + \mathcal{O}(m_\lambda^4).
\end{aligned}
\tag{A7}
$$

In particular, with Eq. (5) and the expressions for N_{3i}^2, the identity (7) is satisfied up to terms of order $\mathcal{O}(m_\lambda^4)$.

[1] V. Silveira and A. Zee, Phys. Lett. **161B**, 136 (1985).
[2] J. McDonald, Phys. Rev. D **50**, 3637 (1994).
[3] C. Burgess, M. Pospelov, and T. ter Veldhuis, Nucl. Phys. **B619**, 709 (2001).
[4] N. Arkani-Hamed, S. Dimopoulos, and S. Kachru, arXiv: hep-th/0501082.
[5] R. Mahbubani and L. Senatore, Phys. Rev. D **73**, 043510 (2006).
[6] F. D'Eramo, Phys. Rev. D **76**, 083522 (2007).
[7] R. Enberg, P. Fox, L. Hall, A. Papaioannou, and M. Papucci, J. High Energy Phys. 11 (2007) 014.
[8] T. Cohen, J. Kearney, A. Pierce, and D. Tucker-Smith, Phys. Rev. D **85**, 075003 (2012).
[9] C. Cheung and D. Sanford, J. Cosmol. Astropart. Phys. 02 (2014) 011.
[10] E. Ma, Phys. Rev. D **73**, 077301 (2006).
[11] S. M. Boucenna, S. Morisi, and J. W. Valle, Adv. High Energy Phys. **2014**, 831598 (2014).
[12] N. G. Deshpande and E. Ma, Phys. Rev. D **18**, 2574 (1978).
[13] R. Barbieri, L. J. Hall, and V. S. Rychkov, Phys. Rev. D **74**, 015007 (2006).
[14] E. Ma, Phys. Rev. Lett. **81**, 1171 (1998).
[15] F. Bonnet, M. Hirsch, T. Ota, and W. Winter, J. High Energy Phys. 07 (2012) 153.
[16] D. Aristizabal Sierra, A. Degee, L. Dorame, and M. Hirsch, J. High Energy Phys. 03 (2015) 040.
[17] D. Restrepo, O. Zapata, and C. E. Yaguna, J. High Energy Phys. 11 (2013) 011.
[18] S. S. Law and K. L. McDonald, J. High Energy Phys. 09 (2013) 092.
[19] T. Toma and A. Vicente, J. High Energy Phys. 01 (2014) 160.
[20] A. Vicente and C. E. Yaguna, J. High Energy Phys. 02 (2015) 144.
[21] T. Abe, R. Kitano, and R. Sato, Phys. Rev. D **91**, 095004 (2015).
[22] S. P. Martin, arXiv:1205.4076.
[23] D. Suematsu and T. Toma, Nucl. Phys. **B847**, 567 (2011).
[24] S. Fraser, E. Ma, and O. Popov, Phys. Lett. B **737**, 280 (2014).
[25] G. Passarino and M. Veltman, Nucl. Phys. **B160**, 151 (1979).
[26] J. Casas and A. Ibarra, Nucl. Phys. **B618**, 171 (2001).
[27] A. Ibarra and G. G. Ross, Phys. Lett. B **591**, 285 (2004).
[28] Z. Maki, M. Nakagawa, and S. Sakata, Prog. Theor. Phys. **28**, 870 (1962).
[29] H. K. Dreiner, H. E. Haber, and S. P. Martin, Phys. Rep. **494**, 1 (2010).
[30] F. Staub, T. Ohl, W. Porod, and C. Speckner, Comput. Phys. Commun. **183**, 2165 (2012).
[31] F. Staub, arXiv:0806.0538.
[32] F. Staub, Comput. Phys. Commun. **185**, 1773 (2014).
[33] W. Porod, F. Staub, and A. Vicente, Eur. Phys. J. C **74**, 2992 (2014).
[34] D. Forero, M. Tortola, and J. Valle, Phys. Rev. D **90**, 093006 (2014).
[35] J. Adam *et al.* (MEG Collaboration), Phys. Rev. Lett. **110**, 201801 (2013).
[36] G. Aad *et al.* (ATLAS Collaboration), J. High Energy Phys. 05 (2014) 071.
[37] W. Beenakker, R. Hopker, and M. Spira, arXiv:hep-ph/ 9611232.
[38] J. M. Cline, K. Kainulainen, P. Scott, and C. Weniger, Phys. Rev. D **88**, 055025 (2013).
[39] U. Chattopadhyay, D. Choudhury, M. Drees, P. Konar, and D. Roy, Phys. Lett. B **632**, 114 (2006).
[40] M. Klasen, C. E. Yaguna, J. D. Ruiz-Alvarez, D. Restrepo, and O. Zapata, J. Cosmol. Astropart. Phys. 04 (2013) 044.

[41] G. Servant and T. M. Tait, Nucl. Phys. **B650**, 391 (2003).
[42] K. Kong and K. T. Matchev, J. High Energy Phys. 01 (2006) 038.
[43] F. Burnell and G. D. Kribs, Phys. Rev. D **73**, 015001 (2006).
[44] J. Edsjo, M. Schelke, P. Ullio, and P. Gondolo, J. Cosmol. Astropart. Phys. 04 (2003) 001.
[45] S. Profumo and A. Provenza, J. Cosmol. Astropart. Phys. 12 (2006) 019.
[46] W. Porod and F. Staub, Comput. Phys. Commun. **183**, 2458 (2012).
[47] G. Belanger, F. Boudjema, A. Pukhov, and A. Semenov, Comput. Phys. Commun. **176**, 367 (2007).
[48] G. Belanger, F. Boudjema, A. Pukhov, and A. Semenov, Comput. Phys. Commun. **192**, 322 (2015).
[49] N. Arkani-Hamed, A. Delgado, and G. Giudice, Nucl. Phys. **B741**, 108 (2006).
[50] D. Akerib *et al.* (LUX Collaboration), Phys. Rev. Lett. **112**, 091303 (2014).
[51] M. El Kheishen, A. Aboshousha, and A. Shafik, Phys. Rev. D **45**, 4345 (1992).